

NASA Contractor Report 172235

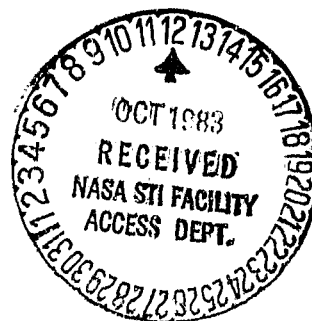
HIGH EFFECTIVENESS LIQUID DROPLET/GAS
HEAT EXCHANGER FOR SPACE POWER APPLICATIONS

{NASA-CR-172235) HIGH EFFECTIVENESS LIQUID DROPLET/GAS HEAT EXCHANGER FOR SPACE POWER APPLICATIONS Interim Report (Washington Univ.) 10 p HC A02/MF A01 CSCL 20D N83-35319
Unclas
G3/34 44081

A. P. Bruckner and A. T. Mattick

UNIVERSITY OF WASHINGTON
Seattle, Washington

Grant NAG1-327
September 1983



NASA
National Aeronautics and
Space Administration
Langley Research Center
Hampton, Virginia 23665

HIGH EFFECTIVENESS LIQUID DROPLET/GAS HEAT EXCHANGER
FOR SPACE POWER APPLICATIONS

ORIGINAL PAGE IS
OF POOR QUALITY

A.P. Bruckner and A.T. Mattick
Aerospace and Energetics Research Program
University of Washington
Seattle, WA 98195

Abstract

A high-effectiveness liquid droplet/gas heat exchanger (LDHX) concept for thermal management in space is described. Heat is transferred by direct contact between fine droplets (~100-300 μ m diameter) of a suitable low vapor pressure liquid and an inert working gas. Complete separation of the droplet and gas media in the zero-g environment is accomplished by configuring the LDHX as a vortex chamber. The large heat transfer area presented by the small droplets permits heat exchanger effectiveness of 0.9-0.95 in a compact, lightweight geometry which avoids many of the limitations of conventional plate and fin or tube and shell heat exchangers, such as their tendency toward single point failure. The application of the LDHX in a high temperature Brayton cycle is discussed to illustrate the performance and operational characteristics of this new heat exchanger concept.

I. Introduction

Heat exchange represents one of the most challenging problems in the design of space prime power systems. Even the most advanced concepts for thermal management in space invoke heat exchanger designs of the conventional plate and fin or tube and shell type, which involve heat transfer through solid surfaces. Such designs are temperature-limited by materials considerations, impose significant pressure drops, and tend to be complex and heavy. They are also susceptible to single point failure. Compromises in heat exchanger effectiveness must usually be made to assure long-term reliability. These problems present serious barriers to the development of successful space power systems.

Studies of internal thermal management in space systems, carried out at the University of Washington, have indicated that the classical limitations of conventional heat exchangers can be circumvented by using direct-contact heat transfer between fine droplets of a low-vapor-pressure liquid and an inert working gas.¹ A device based on this principle, the liquid droplet heat exchanger (LDHX), has been conceived in which a uniform spray of liquid droplets flows countercurrent to a gas and the two media, in direct contact, exchange energy by convection. The large heat transfer area presented by the multitude of droplets permits high heat exchanger effectiveness in a very compact, lightweight geometry.

The avoidance of heat transfer through solid surfaces allows operation of the LDHX at temperatures beyond the capabilities of conventional heat exchangers. Pressure losses are greatly reduced

since the heat transfer media do not have to traverse a multitude of long and narrow passages or tubes. Furthermore, the absence of these components diminishes the chances of single point failure and offers significant reductions in heat exchanger mass.

The principal design requirement of a direct-contact heat exchanger is effective separation of the heat exchange media following heat transfer. To achieve this in the zero-g environment of space, a vortex chamber configuration is proposed for the LDHX in which the swirling gas induces a centrifugal force on radially injected droplets, driving them to the periphery, where they are removed after coalescing into a liquid film. This configuration results in very compact light-weight designs which are suitable for either heating or cooling a working gas in such applications as Brayton cycles or cryogenic cycles.

This paper presents the results of investigations of the LDHX for a power cycle application, i.e., heat addition and heat rejection in a Brayton cycle. The geometry and principle of the LDHX are described first, followed by a review of the choice of droplet media and techniques for the generation of droplets. The application of the LDHX in the Brayton cycle is then discussed and the operational characteristics of the LDHX are presented. Finally, an experimental program to evaluate vortex chamber flow is described.

II. The Liquid Droplet/Gas Heat Exchanger

Several configurations for the LDHX have been investigated, using various principles for separation of droplets and gas in the zero-g space environment.¹ Among the most promising of these is a configuration similar to cyclone dust separators. Cyclone separators are commonly used in earthbased industrial plants and power stations to efficiently and inexpensively separate particulates from dust-laden gases.² Separation is due to swirl of the gas and the resulting centrifugal forces acting on the particulates.

Figure 1 shows a schematic of the proposed LDHX. The working gas is injected tangentially into the chamber through a series of longitudinal inlet ports at the periphery of the chamber, producing a swirling flow.[‡] The gas spirals inward to a central tubular manifold where it exits the chamber through several exhaust ports. The liquid droplets are injected radially outward into the swirling gas from an array of orifices on the walls

[‡]In a practical device the inlet ducts would probably not be discrete, as shown in Fig. 1, but would be part of a scroll-type gas inlet manifold.

of the central manifold. The walls of this component are hollow and function as the liquid injection manifold. The droplets gain tangential momentum from the drag of the gas vortex and are driven outward by the resulting centrifugal force, thus following expanding spiral paths. During their traversal of the LDHX chamber the droplets exchange heat convectively with the working gas. Since the net gas flow is radially inward and the net droplet flow is radially outward the LDHX behaves as a counterflow heat exchanger. Upon reaching the periphery the droplets coalesce into a rotating liquid film which is drawn off through a series of shallow skimmers set into the curved wall. The collected liquid is continuously pumped back to the heat source or heat rejection system, depending on the application of the LDHX.

As indicated above, heat transfer in the LDHX can occur in either direction, i.e., gas can be heated by hot droplets or cold droplets can be used to extract waste heat from a working gas. In the latter case the LDHX can be integrated with a liquid droplet radiator (LDR)^{3,4} so that waste heat is radiated directly by the heat exchanger liquid, in the form of a droplet cloud.

A quasi-one-dimensional, two-phase flow model of the LDHX has been formulated for use in parametric studies aimed at developing practical and effective design configurations. The model includes two continuity equations for the net radial flow of gas and droplets, four momentum equations - one for radial momentum and one for angular momentum for each of the two media - and two energy equations, one for each medium. The volume fraction occupied by the droplets is assumed to be less than 1%. The ideal gas law is assumed and curve fits to tabulated data⁵ are used to determine the viscosity and thermal conductivity of the gas as functions of temperature. The losses caused by shear at the end walls are averaged over the total flow at each radial station, and the losses caused by shear at the cylindrical wall are accounted for by a jet recovery factor which relates the inlet gas velocity to the peripheral velocity of the vortex.⁶ Wall friction at the central manifold is not included, as its effect on the flow is small. The interaction of the droplets and the gas is included as drag terms in the respective momentum equations. The standard drag coefficient curve for single spheres is used.² The wall friction coefficient is determined from the Blasius expression for turbulent flow over a flat plate.⁶ Heat transfer between droplets and gas is assumed to follow the Nusselt number correlation for single spheres.⁷

Secondary flows have not been included as yet. It is well known that in single phase (gas only) confined vortexes wall friction gives rise to secondary flows which, under certain circumstances, such as very low length to diameter ratios and high mass flows, can significantly alter the gas streamline patterns.⁶ In the type of two-phase counter-current vortex considered here the droplets have a first order effect on the gas velocity profiles. The drag of the droplets on the gas is much greater than the drag at the walls of the chamber, and dominates the flow. The tangential gas velocity profile, for example, is substantially different from that of a free or confined pure gas vortex. It is expected that the presence of the droplets will significantly alter the secondary

flow effects but this must be verified by experiments.

The quasi 1-D computations have shown that for a specified power rating, the diameter of an LDHX is governed by many parameters, such as the droplet diameter, density and specific heat, the radial and tangential components of droplet injection velocity, the inlet velocity and thermodynamic properties of the gas, the temperature drops across the two media, the temperature differences between the media, the relative mass flow rates of the two media and the height of the chamber. The interplay of the parameters listed above is complex and has been studied empirically for a variety of potential applications. In general, it appears that droplets in the 100-300 μm range result in LDHX configurations of interest in the majority of cases.

III. Droplet Media and Generation

The droplet material must remain liquid in the range desired for an operating temperature. It must also be inert at high temperature with respect to the working gas and should have a low vapor pressure ($<2 \times 10^{-4}$ torr) to avoid contamination of the gas in the heat exchanger. Liquid metals and eutectic alloys in contact with noble gases generally meet these criteria for temperatures above about 350°K.⁸ For temperatures above 505°K and up to ~1300°K tin appears to be the most suitable material due to its extremely low vapor pressure.⁹ For temperatures in the 350-600°K range a variety of low melting point eutectic alloys are available.³ Lithium is suitable between 470°K and 600°K and silicone oils could be used in the 270-350°K range. The media suitable for lower temperature applications would be used in heat rejection applications. These same media have been considered for use in the liquid droplet radiator concept.^{3,4}

Proper operation of the LDHX requires that droplets be neither carried out of the device with the gas stream nor be allowed to leave the heat exchanger without having exchanged the desired amount of thermal energy with the gas. The heat capacity, heat transfer rate, and total transit time of droplets in the heat exchanger depend strongly on the properties of the droplet material, droplet size, droplet injection velocity and tangential gas velocity profile. The generation of uniform droplets is essential for optimal LDHX design and operation, particularly in the zero-g environment.

Practical techniques exist which can be used to produce uniformly sized droplet streams in a heat exchanger.^{10,11} The liquid medium is injected through a large number of small orifices and the resulting streams caused to break up into a series of uniform drops by inducing regular perturbations in the emerging jets with a vibrator.¹¹ Such a scheme is used in ink-jet printers to produce accurately aimed streams of droplets $<50 \mu\text{m}$ in diameter at rates up to 10^5 Hz.¹² Experimental studies of droplet formation with mercury and silicone oils, carried out at the University of Washington, have demonstrated that excellent control of droplet size and spacing can be easily achieved by acoustically driving the injector plenum with a piezoelectric crystal.⁴ Figure 2 shows photographs of mercury droplet streams (200 μm droplet diameter) with and without

ORIGINAL PAGE IS
OF POOR QUALITY

acoustical drive. Similar results have been obtained with silicone oils.

It should be noted at this point that, for those LDHX applications involving liquid metals, the compatibility of the liquid metals with the materials of the pumping system and heat exchanger has to be carefully considered. Components exposed to liquid metal contact must be made of, or protected by, materials resistant to corrosion, such as tungsten, molybdenum, zirconium or alloys thereof.⁸ In each application range materials compatibility must be an important aspect of the design.

IV. Sample Applications

Since the performance, specific mass, and long-term reliability of space Brayton cycles are largely governed by the corresponding parameters of the cycle's heat exchangers, it was felt that this is an application area where the liquid droplet heat exchanger could have a significant beneficial impact. Indeed, a primary aim of our research program is to investigate the potential use of the LDHX in Brayton cycles and to develop LDHX configurations of practical interest. To illustrate an example, we present here the results of numerical calculations for two liquid droplet heat exchangers, one intended for the heat addition loop of a Brayton cycle and the other for the heat rejection loop of the same cycle, as shown in Fig. 3.

Brayton Cycle Parameters

For present purposes a 100 KW_e regenerative Brayton cycle was chosen, modeled after a system developed by AiResearch-NASA Lewis.¹³ Liquid droplet heat exchangers and a liquid droplet radiator have been substituted for the conventional heat exchangers and radiator normally assumed for Brayton cycles. A conventional recuperator having an effectiveness of 0.92 was assumed for the time being; however, the possible use of droplet heat exchangers for this application is currently under study. (An LDHX recuperator would require two separate LDHX chambers to transfer heat between the hot and cold gas streams.)

The relevant cycle parameters are illustrated in Fig. 3. Although the LDHX is capable of operating at temperatures up to 1300°K¹ (this limit is determined by the maximum acceptable vapor pressure of tin, i.e., $\sim 2 \times 10^{-4}$ torr at 1300°K), the more modest turbine inlet temperature of 1100°K was chosen to be consistent with current state of the art. All other cycle parameters, such as component efficiencies, are also within the state of the art. The source of heat has not been specified but could, for example, be a liquid metal cooled nuclear reactor.

The pressure drop in the recuperator was assumed to be 3% for both the hot and cold sides. The gas pressure drop in the hot LDHX turned out to be less than 0.1% but was assumed to be 0.5% in the cycle calculations to account for pressure drops in

*The very low pressure drops are a result of the low gas flow velocity and droplet loading in the two devices. For example, the maximum tangential velocity of the gas in either device is only 1/3 to 1/10 of that found in typical cyclone separators.

ORIGINAL PAGE IS OF POOR QUALITY

the gas manifolds. Similarly, for the cold LDHX the pressure drop was taken to be 1%.* Under these conditions the thermal efficiency of the cycle is 39.3%. This high efficiency is largely a result of the low heat rejection temperature made possible by the use of an LDR. If conventional heat exchangers with typical pressure losses of 3% are assumed, the cycle efficiency is 36.1%. Thus the use of droplet heat exchangers results in an improvement of cycle efficiency of more than three percentage points.

LDHX Parameters and Results

The working gas is a mixture of 72% He and 28% Xe (molecular weight = 39.6) and is heated at 10 atm by molten tin droplets injected into the high temperature LDHX at 1125°K. The gas inlet and exit temperatures are 831°K and 1100°K, respectively. The tin leaves the device at 856°K. Assuming an alternator efficiency of 0.95, the hot LDHX must transfer 268 KW_{th} for a net electrical power output of 100 KW_e . For a liquid/gas thermal capacitance ratio of 1.0 this thermal power level requires a mass flow of tin of 3.84 kg/sec and a mass flow of gas of 1.9 kg/sec.

In the heat rejection LDHX, droplets composed of Dow 705 silicone oil are injected at 280°K. The gas inlet and exit temperatures are 464°K and 300°K, respectively, and the gas exit pressure is 4.80 atm. The oil is heated to 344°K and pumped to the liquid droplet radiator. To reject the 163 KW of waste heat an oil mass flow rate of 1.82 kg/sec is required.

For the conditions summarized above, a parametric study for each LDHX has been carried out for a range of droplet sizes (100-300 μm), injection velocities (5-10 m/sec), chamber heights (10-25 cm), central manifold diameters (10-20 cm) and tangential gas velocities at the central manifold (5-20 m/sec). Table I summarizes the input parameters and pertinent results for the hot and cold LDHX for one set of cases. The results presented in these examples have not been optimized but do reflect practical designs which are being examined further.

The small dimensions of the LDHX chambers are particularly noteworthy. The external dimensions of the devices will be somewhat greater due to the presence of structural elements and the liquid and gas manifolds. Further reductions in size appear possible through judicious choice of operating parameters. Since detailed designs for the LDHX and associated components have not yet been developed for the applications presented here, an accurate assessment of specific masses is difficult to make at this time. As a first estimate, it is reasonable to assume an LDHX mass equal to that of the outer pressure shell of a conventional heat exchanger of equal thermal capacity. Because the LDHX does not incorporate the complex internal plumbing of a conventional heat exchanger, its specific mass may be as low as one-tenth of that of an equivalent conventional heat exchanger.

Velocity and temperature profiles in the two devices are shown in Figs. 4-5. In both cases the tangential gas velocity profiles are markedly different from those of a free vortex, particularly in the hot LDHX (Fig. 4). The tangential velocity of the gas in the hot LDHX decreases rapidly immediately upon entering the chamber periphery.

This is due to the drag exerted by the liquid metal droplets on the gas. As the gas spirals in, its tangential velocity reaches a minimum approximately halfway to the central manifold and then begins to increase as the conservation of angular momentum overcomes the drag of the droplets. The inward radial component of gas velocity increases faster than the inverse of the radius, because the gas density decreases with decreasing radius as a result of the heating. Following the droplets outward from the central manifold one sees that their tangential velocity at first decreases with increasing radius, approximately following the slope of the tangential gas velocity curve. About midway to the periphery, where the droplets begin to see an increase in the tangential gas velocity, the droplet tangential velocity increases also as a result of the increasing drag of the gas on the droplets. The radial velocity of the droplets, after a slight increase near the manifold, decreases with increasing radius for a considerable distance. This is due to the fact that over much of the radial dimension of the chamber the radial drag component on the droplets exceeds the centrifugal force. It is only where the tangential velocity of the droplets begins to significantly increase, thus increasing the centrifugal force, that the droplets undergo a radial acceleration.

The temperature profiles in the hot LDHX reflect the dynamic behavior of the gas and droplets. The steepening of the slope of the temperature profiles with increasing radius is a result of the diminishing radial velocity of the droplets.

In the cold LDHX, the droplets have less influence on the gas dynamics. The tangential gas velocity increases monotonically with decreasing radius, though much more slowly than in a free vortex or even a pure gas vortex in the same chamber. It is evident that the drag of the silicone oil droplets is not sufficient to cause the radical changes observed in the hot LDHX. This difference in the dynamics of the hot and cold devices is largely due to the much lower density (1.09 g/cm^3) and much higher specific heat ($0.334 \text{ cal/g}^\circ\text{K}$) of the oil droplets relative to the tin droplets (6.8 g/cm^3 ; $0.062 \text{ cal/g}^\circ\text{K}$ respectively).

It is well known that liquid droplets injected into a gas stream will shatter if the aerodynamic forces acting on the droplets are sufficiently high.¹⁴ Such a situation is naturally to be avoided in an LDHX. In the sample cases presented here, the slip velocity between the gas and droplets is low enough at all radii that no aerodynamic droplet breakup occurs in either device. Similarly, the collision dynamics of the droplets with the rotating liquid film at the periphery of the chamber is such that no splashing occurs. Estimates of liquid film thicknesses at the periphery indicate that in the hot LDHX the film of liquid tin will build up to a maximum of $\sim 0.5 \text{ mm}$ at each skimmer and in the cold LDHX the maximum oil film thickness will be $\sim 0.8 \text{ mm}$.

Evaporation Losses

The choice of a droplet medium for a given temperature range is largely determined by the necessity to avoid significant contamination of the working gas and to minimize the loss of droplet

material through evaporation. Both these requirements dictate the use of materials having very low vapor pressures. Since the decrease of vapor pressure with decreasing temperature is very steep for all media of interest, most of the evaporation occurs at the hot end of the droplet heat exchanger.

Consider the vaporization of tin in the high temperature LDHX. Assuming that the working gas leaving the heat exchanger is saturated with tin at the vapor pressure corresponding to the highest droplet temperature (1125°K),* the volume flow rates of tin vapor and working gas will be in the same ratio as their respective partial pressures, P_{Sn} and P_{g} . In the present case $P_{\text{Sn}} = 3.5 \times 10^{-6} \text{ torr}^9$ and $P_{\text{g}} = 10 \text{ atm}$. Assuming ideal gas behavior it can be shown that the mass flow rate of tin vapor out of the LDHX is only $2.5 \times 10^{-9} \text{ kg/sec}$. For a 5 year lifetime this amounts to an evaporation of only 0.4 kg of tin.

Since the vapor is trapped in the closed gas loop the tin is not lost from the system. The vapor will condense in the colder components of the system. If the vapor pressure of the tin were to remain in equilibrium with the gas temperature, virtually all of it would condense in the turbine. However, because of the rapidity of the gas flow through the turbine, the tin vapor would likely be supercooled and condense downstream of the turbine as a very dilute mist of submicron droplets which would be entrained in the gas flow.

The evaporation loss of the silicone oil in the low temperature LDHX can be calculated in the same manner as above. The vapor pressure of the oil at 344°K is $2.8 \times 10^{-7} \text{ torr}^{15}$ and its molecular weight is 546, thus the mass loss rate of oil is calculated to be $1.7 \times 10^{-9} \text{ kg/sec}$ or 0.27 kg over 5 years, again a trivial amount.

Liquid Pumping Power Requirements

The power required for injection of the liquids into the two heat exchangers was calculated by assuming laminar flow through capillary orifices having length to diameter ratios of 3.5. The power required for tin injection is 383 W and for oil injection it is 254 W.

The transport losses in interconnecting pipes were calculated by assuming turbulent pipe flow for both the tin and the oil. Assuming a smooth pipe of 2.5 cm dia \times 5 m long for each liquid loop,** the power required to overcome pipe friction is $\sim 45 \text{ W}$. Thus, the combined injection and transport losses amount to only $\sim 682 \text{ W}$ or $\sim 0.7\%$ of the net power output of the Brayton cycle.

*The gas will actually be supersaturated with tin vapor because the gas temperature is 25°K colder than the droplet temperature.

**Only that part of the oil loop in the immediate vicinity of the LDHX has been included. The actual length of piping for oil transport is greater than 5 m but is considered part of the LDR system.

V. Experimental Program

The quasi-one-dimensional analysis described earlier in this paper is only the first step in our understanding of the gas and droplet dynamics in the LDHX. The model is based on a number of assumptions whose validity must be checked with experimental observations. Of particular interest is the nature of secondary flows and their effect on the gas and droplet streamlines.

A small-scale vortex chamber is being built for the purpose of investigating the two-phase flow dynamics of the LDHX. This first experimental device does not involve heat transfer. Figure 6 shows a photograph of the partially completed vortex chamber. The top and bottom plates of the device are made of Plexiglas to permit flow visualization studies. One of the plates will be equipped with an array of pressure taps to measure the radial static pressure profile in the flow. The central manifold has a diameter of 7.8 cm and the outer wall of the chamber has a diameter of 28 cm. The height of the chamber is 5.0 cm. The working gas is air and is injected into the chamber at 1-2 atm pressure through four equally-spaced 0.6 cm x 5.0 cm longitudinal ports at the chamber periphery. A concentric gas plenum chamber surrounds the vortex chamber. The gas flow rate is controlled by a sonic orifice in the gas supply line.

Initial tests will be carried out with water and/or ethylene glycol as the droplet medium. Eventually, silicone oils, and possibly mercury, may be used. Figure 7 is a photograph of the central droplet-injector/gas-exit manifold. The liquid is injected from small orifices (100 μ m dia) drilled in the sides of 3.2 mm O.D. brass tubes which are held in grooves machined in the manifold wall. There are 24 such tubes (for clarity only 6 are shown in Fig. 7), each one with 15 equally spaced orifices, for a total of 360 injector orifices. Each injector tube can be rotated $\pm 45^\circ$ about its own axis to allow the injected droplets to be imparted a tangential velocity component as well. The liquid flow rate is measured by a rotameter in the liquid feed line. Acoustic excitation for uniform droplet generation will be provided by a piezoelectric transducer (not shown) attached to the closed end of the central manifold.

Figure 7 also shows the gas exit ports. The gas is exhausted from the bottom of the manifold and is directed to a back pressure control valve. The liquid film which forms at the periphery of the vortex chamber is removed by means of four skimmer slits (adjacent to the gas inlet ports) whose configuration is similar to that illustrated in Fig 1. The spent liquid is collected for re-use.

Gas flow parameters in the vortex chamber will be measured using pitot and static pressure probes, static wall pressure ports and boundary layer probes. Secondary flow effects will be observed by a flow visualization technique similar to that for visualizing the droplet flow, described below.

Droplet dynamics will be visualized by a streak velocimetry technique.¹⁶ The liquid will be doped with a strongly fluorescent dye such as Rhodamine 6G, and the swirling two-phase flow field will be illuminated by an expanded argon-ion laser beam which will be chopped temporally. The

droplets will thus be illuminated by a pulsed light source and will fluoresce only during those times that the chopper lets the laser beam through. A camera will record the moving droplets as fluorescing streaks. These streaks will define the local droplet streamlines. From a knowledge of the duration of the laser pulse, the streak lengths will yield the droplet velocities at any point in the flow. This technique will also permit an assessment of the effects of turbulence on the droplet dynamics and the existence of droplet collisions or breakup. An aspect of the liquid injection process which will receive particular attention is the interaction of the emerging liquid jets with the crossflowing gas stream and the effect of this crossflow on the droplet formation process.

The gas flow will be similarly visualized by seeding the gas with a suspension of very fine particles, such as talcum powder.¹⁶ Because the flow velocities in the device will be relatively low, the very small (5-10 μ m) talcum particles will be in velocity equilibrium with the gas flow. The pulsed laser light scattering off the talcum particles will produce streaks on a photograph of the flow, as described above.

Finally the impingement of the droplets with the chamber periphery and the breakup of the liquid film will be studied using both the flow visualization technique and an electrical conductance film depth probe. The effect of skimmer height on the efficiency of liquid removal will be investigated.

VI. Conclusions

This study shows that direct contact heat exchange between a gas and a liquid heat transfer medium dispersed into fine droplets offers an attractive new approach to thermal management in space. The ability of a liquid droplet heat exchanger to transfer heat directly from a liquid to a working gas over a wide temperature range avoids many of the limitations of conventional heat exchangers such as their tendency toward single point failure. The droplet heat exchanger offers a large surface to volume ratio, a very low gas pressure drop, and high effectiveness in a compact, lightweight geometry.

It is expected that droplet heat exchangers can be developed using available technology. Considerable work is required on a variety of technical problems to develop a practical device, however. These problems include investigation of the details of secondary flows in the two-phase vortex, the detailed design of the gas and liquid inlet and outlet manifolds, the droplet injector, and the liquid film skimmers, and the need to examine material compatibility problems. These and other problems are currently being addressed in a program of theoretical and experimental research on the liquid droplet heat exchanger at the University of Washington.

**ORIGINAL PAGE IS
OF POOR QUALITY**

**ORIGINAL PAGE IS
OF POOR QUALITY**

Acknowledgments

This work was supported by NASA Grant NAG1-327. The authors are deeply indebted to A. Hertzberg without whose support and encouragement this work would not have been possible. Thanks are also due to D.W. Bogdanoff for many helpful discussions.

References

1. A.P. Bruckner and A. Hertzberg, "Direct-Contact Droplet Heat Exchangers for Thermal Management in Space," Proc. 17th Inter-society Energy Conversion Engineering Conference, 107 (1982).
2. W. Strauss, Industrial Gas Cleaning, 2nd ed., Pergamon Press, Oxford, 1976.
3. A.T. Mattick and A. Hertzberg, "Liquid Droplet Radiators for Heat Rejection in Space," J. Energy 5, 387 (1981).
4. A.T. Mattick and A. Hertzberg, "The Liquid Droplet Radiator - an Ultralightweight Heat Rejection System for Efficient Energy Conversion in Space," Acta Astronautica 9, 165 (1982).
5. N.B. Vargaftik, Tables of the Thermophysical Properties of Liquids and Gases, John Wiley & Sons, New York, 1963.
6. W.S. Lewellen, "A Review of Confined Vortex Flows," NASA CR-1772, 1971.
7. J.F. Davidson and D. Harrison, Fluidization, Academic Press, New York, 1971.
8. R.N. Lyon, ed., Liquid-Metals Handbook, U.S. Office of Naval Research, 1954.
9. An. N. Nesmeyanov, Vapor Pressure of the Elements, Academic Press, New York, 1963.
10. J.P. Anno, The Mechanics of Liquid Jets, D.C. Heath & Co., Lexington, MA, 1977.
11. R.H. Wickemeyer and A.K. Oppenheim, "Breakdown of a Liquid Filament into Drops Under the Action of Acoustic Disturbances," Technical Note No. 1-67, Report No. AS-67-6, University of California Office of Research Services, Berkeley, CA, 1967.
12. L. Kuhn and R.A. Myers, "Ink Jet Printing," Sci. Am. 240, 162 (1979).
13. J.E. McCormick and J.H. Dunn, "NASA 30,000 Hour Test Demonstration of Closed Brayton Cycle Reliability," AIAA Paper 77-499 (1977).
14. Dow-Corning Bulletin 22-287, August 1974.
15. S.A. Krzeczkowski, "Measurement of Liquid Droplet Disintegration Mechanisms," Int. J. Multiphase Flow 6, 227 (1980).
16. G.W. Sparks, Jr. and S. Ezekiel, "Laser Streak Velocimetry for Two-Dimensional Flows in Gases," AIAA J. 15, 110 (1977).

Table I. LDHX Parameters

| | Hot LDHX | Cold LDHX |
|---|----------|-----------|
| Droplet Dia. (μm) | 150 | 300 |
| Droplet Injection Velocity Components (m/sec) | | |
| Radial | 7 | 5 |
| Tangential | 7 | 5 |
| Tangential Gas Velocity at Central Manifold (m/sec) | 10 | 15 |
| Central Manifold Dia. (cm) | 10 | 10 |
| Height of Chamber (cm) | 20 | 12.5 |
| Diameter of Chamber (cm) | 61.6 | 31.2 |
| Size of Gas Inlet Ports (cm) | 1.9x20 | 3.58x12.5 |
| No. of Gas Inlet Ports | 8 | 8 |
| Diameter of Injector Orifices (μm) | 80 | 168 |
| No. of Injector Orifices | 11,440 | 10,660 |
| Orifice Spacing (mm)* | 1.91 | 1.72 |
| LDHX Effectiveness | 0.92 | 0.89 |

*It was assumed that 2/3 of the surface area of the central manifold is available for droplet injection and that the orifices are arranged in a square pattern.

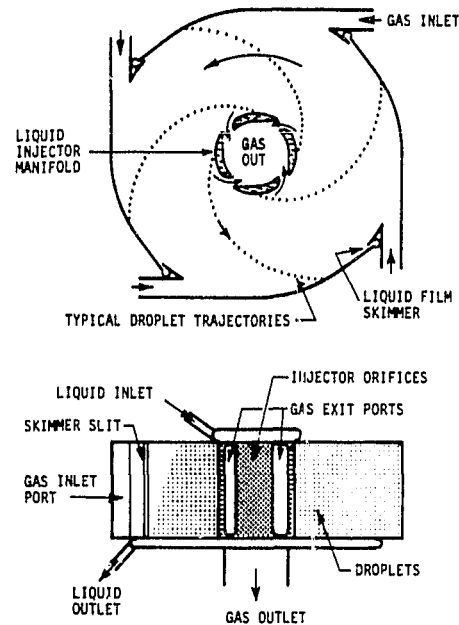


Fig. 1. Schematic of vortex-type liquid droplet/gas heat exchanger. (Only four droplet trajectories shown for clarity).

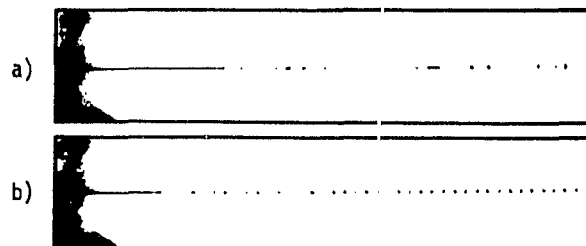


Fig. 2. Mercury droplet streams, generated (a) without acoustic drive, (b) with 9 kHz acoustic drive (droplet diameter $\approx 200 \mu\text{m}$).

ORIGINAL PAGE 13
OF POOR QUALITY

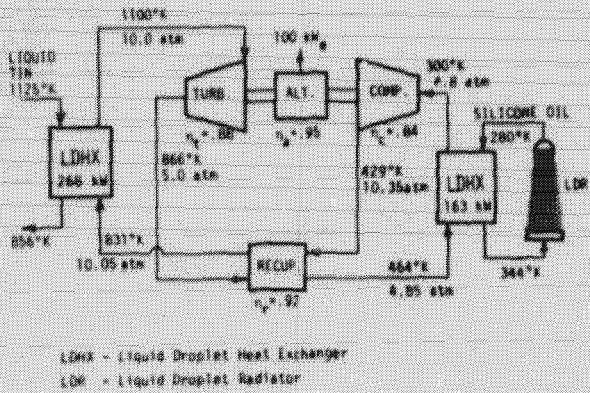


Fig. 3. Brayton cycle utilizing liquid droplet heat exchangers and a liquid droplet radiator (working gas is 72% He, 28% Xe).

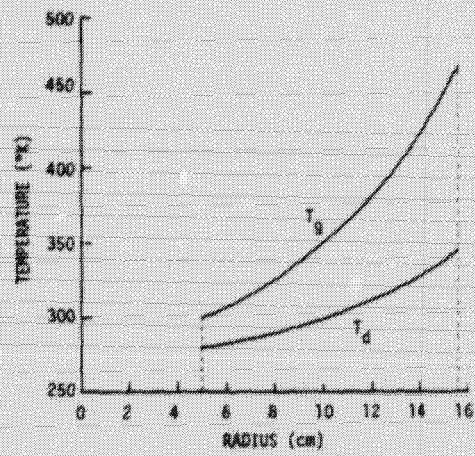
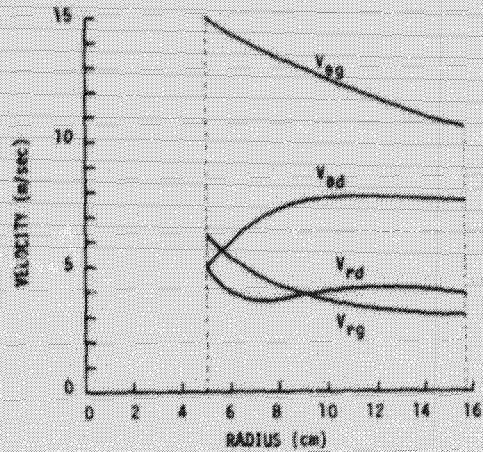


Fig. 5 Velocity and temperature profiles in 163 kW low-temperature LDHX. Subscripts d and g denote droplets and gas, respectively; r and θ denote radial and tangential components. Pressure = 4.8 atm, droplet material is Dow 705 silicone oil, droplet dia. = 300 μ m, chamber height = 12.5 cm. Dotted lines indicate central manifold and chamber periphery.

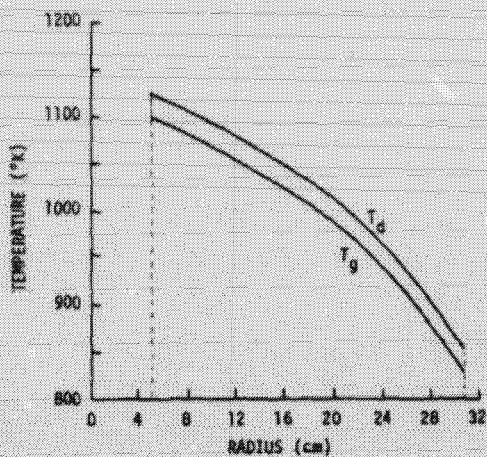
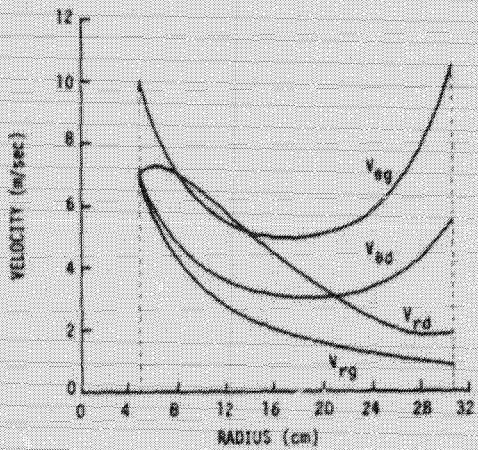


Fig. 4 Velocity and temperature profiles in 268 kW high temperature LDHX. Subscripts d and g denote droplets and gas, respectively; r and θ denote radial and tangential components. Pressure = 10 atm, droplet material is tin, droplet dia. = 150 μ m, chamber height = 20 cm. Dotted lines indicate central manifold and chamber periphery.



Fig. 6. Photograph of experimental droplet/gas vortex chamber.

ORIGINAL PAGE IS
OF POOR QUALITY

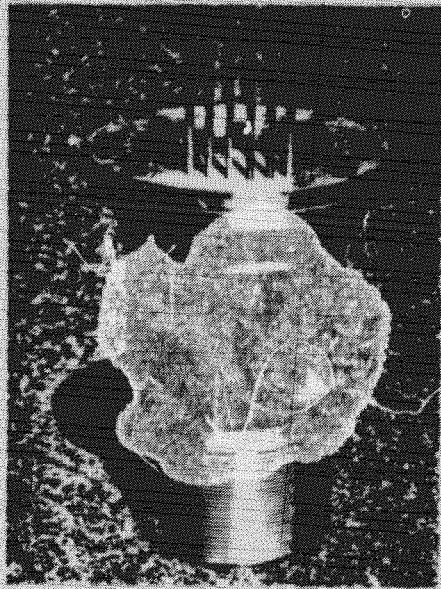


Fig. 7. Close-up of central manifold of experimental vortex chamber, showing several liquid injector tubes and gas exit ports.